

STUDYING THE STRUCTURAL, ELECTRICAL, AND MAGNETIC CHARACTERISTICS OF ASiNRS-DOPED NEODYMIUM USING THE FIRST PRINCIPLE

Thanh Tung Nguyen^{a*}, Thanh Xuan^b

^aInstitute of Southeast Vietnamese Studies, Thu Dau Mot University, Thu Dau Mot City, Binh Duong Province, Vietnam

^bOffice of science, Thu Dau Mot University, Thu Dau Mot City, Binh Duong Province, Vietnam

Article history

Received

28 May 2023

Received in revised form

10 January 2024

Accepted

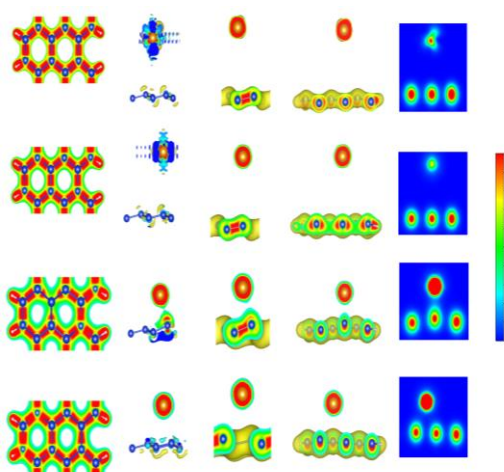
17 January 2024

Published Online

23 June 2024

*Corresponding author
nttung@tdmu.edu.vn

Graphical abstract



Abstract

There have been many applied studies on Nd in medicine, cooling techniques due to large amplitude changes in specific heat capacity, making glass pigments, making laser materials, and many other fields. However, there have been no specific studies on the structural and electronic properties related to the band gap. In this study, we investigated the optimization of Nd adsorption on Armchair nanoribbon silicene substrate. The research was carried out in three steps. The first step is to change the Nd atom through the four positions (top, valley, hollow, and bridge) to determine the optimal position. As a result, the bridge site has a magnetic moment of $4.68 \mu_B$ and a locking degree of 0.69 \AA , has the lowest absorbed energy value of -2.6 eV , and has the most stable structure. Second step, we varied the Si-Si bond length of silicene for the same target, resulting in choosing the optimal bond length of 2.27 \AA . Finally, we consider the distance between the Nd atom and the silicene surface and determine that with the same bond length 2.27 \AA , the result obtained at a height of 2.11 \AA occurs most optimally. This result proves that silicene-doped Nd is very promising as a material for making visible sensors and spin motors in the future.

Keywords: Nd adsorption SiNRs, spintronic material, optoelectronic material, new materials

© 2024 Penerbit UTM Press. All rights reserved

1.0 INTRODUCTION

The 3D structures of silicon blocks and 1D silicone fibers, or 0D silicon materials, were studied several decades ago [1, 2]. However, the basic 2D structure of Si was predicted in 1994 [3]. Beginning with the experimental synthesis of the first 2D graphene in 2004 [4], since then, this 2D Si structure has received considerable attention. The material that is most closely related to graphene is 2D silicon, known as silicene [5]. Silicene has a hexagonal structure analogous to graphene and has no elasticity, but silicene is low-elastic, has many superior characteristics than graphene, and is also easily compatible when replacing Si for C in

semiconductor electronic components. The Si-Si bonds contain hybrid sp^2/sp^3 orbits [6], the mechanism of orbital breeding for the sp^2 mixture. Despite the fact that both silicene and graphene have a Dirac conic structure, which is made up of low-energy pz trajectories, this sp^2/sp^3 shows a similar and relatively weak division of the bonds in silicene compared to the sp^2 -combination of graphene [7]. Due to the fact that the Si element in nature does not appear in layer structures like graphite, silicene can only be synthesized experimentally using the bottom-up epitaxy method [8]. Silicon has many applications, such as field-effect transistors (FETs), temperature sensors, energy storage devices, and the effects of quantum spin hall [9-16].

Due to the similarity of the 2D material with graphene and its compatibility with Si-based electrical devices, silicene could be a viable 2D candidate to replace graphene. However, the narrow bandwidth of silicene restricts its use in nanoelectronics [17]. The expansion of the EG forbidden energy zone for silicone has recently emerged as an exciting field of research that has attracted a lot of attention. Atomic compounding (algae, non-metals, metals, rare earth elements, etc.) is a powerful technique to dramatically change the basic properties of 1D ASiNRs from the point of view of chemical change. The variation in different concentrations and distributions of atoms may be the result of this doping technique [18-25]. Rare-earth intermetallics, also known as lanthanide elements, play an important role in the study of magnetic materials and the development of semi- and super-conducting materials [26]. There have been authors who have studied the radiation properties of Nd with Zeeman splitting at moderate magnetic fields (up to 334 G) of 20 lines of Nd II, covering the part 569.89 nm to 617.05 nm of the visible spectral range [27]. There are authors presented the results of an experimental study designed to explore the electrical properties at the Nd-doped Si-SiO₂ interface [28]. Photoluminescence (PL) properties of the SiOx: Nd thin films were studied as a function of the silicon excess, the annealing temperature and the Nd content [29]. The incorporation of neodymium within silicon nanowires was achieved by using powder as the doping source [30], and permanent magnets [31], laser materials and more other applies [32-36].

However, there has not been any simulation study using the DFT method to investigate the structural and electronic properties of Nd doped with silicene, which we are interested in in this project.

2.0 METHODOLOGY

The structural and electrical characteristics of Nd-adsorption silicene nanoribbons are investigated using the DFT method. All calculations are finished using the VASP software package. The many-body exchange and correlation energies, which are obtained from electron-electron Coulomb interactions, are calculated using the Perdew-Burke-Ernzerhof (PBE) functional. Additionally, the intrinsic electron-ion interactions are characterized by the projector-augmented wave (PAW) pseudopotentials. This set of plane waves has a 400 eV kinetic energy cutoff, which is more than enough to analyze Bloch wave functions and electronic energy spectra. The DFT method is used to look into the structural and electrical characteristics of Nd-adsorption silicene nanoribbons. The VASP software suite is used to conduct all of the calculations. The Perdew-Burke-Ernzerhof (PBE) functional is used to determine the energies for the many-body exchange and correlation processes, which are derived from electron-electron Coulomb interactions. The projector-augmented wave (PAW) pseudopotentials can also be

used to represent the fundamental electron-ion interactions.

$$\Delta E = E_S - E_M - E_P \quad (1)$$

where E_M , E_P , and E_S are the total energy of Nd atom, ASiNRs, and Nd adatom adsorbed on ASiNRs.

3.0 RESULTS AND DISCUSSION

3.1 Structural Properties

It is shown how to construct a survey model using a monolayer ASiNRs model with N of 6 (see Figure 1). The model uses Nd as the sturdy metal, and its basic structure consists of 12 C and 4 H atoms. We set up four Nd adsorption models based on ASiNRs: valley, top, bridge, and hollow positions (see Figure 1).

The first step, the results record in Table 1.

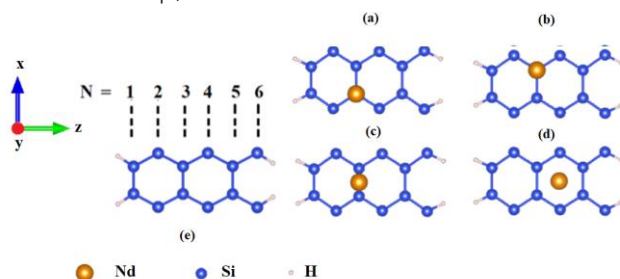


Figure 1 Structures of (a) Valley, (b) Top, (c) Bridge (d) Hollow, (e) Pristine

Based on Table 1, we see through the calculation results that we have obtained values such as the formation energy of metal E_M , the formation energy of substrate SiH, and the energy of formation of substrate (E_P) ASiNRs. Formation of the absorption system including ASiNRs(M_P) and Nd (E_M). Besides, there are calculation results of buckling, the height of metal atom Nd on the surface compared to pristine, bond angle between 3 nearest atoms Si-Si-Si, and moment value. From Mag, the structural states consider the stability of the bonds after adsorption together between the Nd metal and the pristine substrate surface ASiNRs. Through Table 1, we look at the initial substrate ASiNRs as a basis so that after metal adsorption we have new results, through which we can compare all the similar and different properties. Specifically, in the case of pristine substrate ASiNRs with configuration N = 6. Originally a semiconducting compound, non-magnetic, with formation energy - 69.56 eV, has a buckling of 0.44 Å, bond-angle between 3 Si atoms is 116°29', the band gap of 0.33 eV.

Table 1 Table of results for calculating and structuring states of the 4 positions

Vị trí	Valley	Top	Bridge	Hollow	Pristine
E_P (eV)	-69.56	-69.56	-69.56	-69.56	-69.56
E_M (eV)	-2.61	-2.94	-2.60	-2.48	x
E_s (eV)	-74.26	-74.27	-74.76	-74.56	x
ΔE (eV)	-2.09	-1.76	-2.60	-2.52	x
Buckl (Å)	0.40	0.40	0.69	0.38	0.44
Angle	117°06	117°06	115°53	117°27	116°28
Mag (μ)	3.86	3.86	4.68	4.28	0.00
E_g (eV)	0	0	0	0	0,33
States	H	H	H	H	H

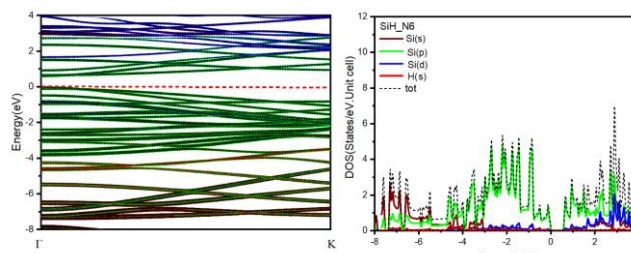
After calculating, we immediately commented on the results and found that: the positions (top, valley, hollow, bridge) all have stable configurations (H - High), equally stable. However, when we consider and compare the cases there are differences in detail, through which we can see which position gives the best result we expect. According to the results of Table 1, the Bridge position has the lowest value of absorbed energy, which can be understood as the most stable, with the strongest magnetic moment of 4.68 μ_B and relatively high buckling of 0.69 Å; The Si-Si-Si bond angle at this time 115°28' is also close to the pristine case where this angle has a value of 116°27'. The above factors show that the Bridge position is considered an effective position. most effective compared to the remaining sites when allowing Nd to absorb ASiNRs.

In the second step, we conduct an investigation at the same bridge position but with different assumed initial bond lengths f_0 of Si-Si from 2.25 Å to 2.5 Å to find out what the distance between Si-Si atoms is. how much for the best adsorption to occur for Nd atoms. The results show that at a stable Si-Si bond length of 2.27 Å (initial 2.35 Å) the optimal level is reached with the bond energy at the lowest level of -5.3 eV. Besides, in Table 2 we see that the corresponding bond lengths 2.3 Å and 2.29 Å (original 2.4 Å and 2.45 Å, respectively) have lower energies of -5.53 eV and -5.79 eV but the structure of they are conversely unstable compared to the chosen case.

Finally, we consider the distance between the Nd atom and the silicene surface, with the initial assumption that Nd relative to the silicene surface (the plane containing 3 Si atoms at the top position) has a height of 4.5 Å to 7.5 Å. Through calculations, with the same bond length of 2.27 Å, the result obtained at a height of 2.11 Å has the most optimal adsorption energy, while still ensuring a stable structure

3.2 Structural Properties

When considering the energy band structure of the ASiNRs substrates, we obtained the results as shown in Figure 2.

**Figure 2** (a) Pristine DOS structure, (b) Pristine band structure

According to the energy band structure in Figure 2 drawn from the ASiNRs on Origin software, when choosing the Fermi energy level equal to 0 eV, through the calculation results, we can see the characteristic strongly active electron orbitals of ASiNRs here are Si(s) in wine, Si(p) in green, Si(d) in blue, and H(s) in red; The band gap energy value of pristine is $E_g = 0.33$ eV. At that time, the Si(s) orbitals usually have high energy and are located deep at the bottom of the valence band (from -5eV to -8 eV). The Si(p) orbital electrons are concentrated in both the conduction band (above the fermi level) and the valence band (below the fermi level). The band gap E_g of the studied material is formed from these orbital electrons. According to Figure 4, the DOS state density of the obtained ASiNRs shows that the Si(s) orbital electron energies are relatively strong compared to Si(p) and Si(d), the energy value of Si(s) level is about 3.5 ~ (states/eV) and is strongest in the -5 eV to -1 eV region. The electronic energy of Si(p) are strong, location at all the valence band (from -7.5 eV to 0 eV) and bottom of the conduction band from 0.33 eV to 3 eV, orbital electron energies Si(d) stay at 0.5 eV to 4 eV.

In the pristine state, the H(s) electronic energy contributes to the formation of band structure, but at a very small level and can be ignored. In the case of pristine H(s), it exists around -4 eV in the middle of the valence band.

Table 2 Calculation results when changing bond-length

d_0 (Å)	2.25	2.30	2.35	2.40	2.45	2.50
Si(eV)	-69.36	-69.60	-69.73	-69.56	-69.70	-69.56
Nd(eV)	-2.20	-3.46	-2.41	-1.99	-1.93	-2.61
Nd/Si (eV)	-77.91	-77.34	-77.45	-77.08	-77.42	-74.27
Delta (eV)	-6.36	-4.29	-5.30	-5.53	-5.79	-2.09
Mag(μ)	3.84	4.00	3.86	3.96	3.81	3.86
Buckl (Å)	0.20	0.44	0.41	0.38	0.42	0.46
Angle	111°5	110°2	111°6	110°4	112°0	117°1
Si-Si (Å)	2.26	2.26	2.27	2.30	2.29	2.29
States	L	M	H	L	M	H

Based on Figure 3, and Figure 4, we represent the electron orbitals with corresponding colored lines Si(s) in green; Si(p) in dark-green; Si(d) in light-green; Nd(s) in orange; Nd(p) in pink; Nd(d) in Ink-blue; Nd(f) in red. Considering Figure 3, the electronic band structures of the Nd metal absorption cases on the ASiNRs semiconductor background at different positions are different top, valley, bridge, and hollow. They have in common that after absorbing the Nd atom the electronic orbitals near the Fermi level for pristine ASiNRs that are semiconductors now have an overlap between the valence and conduction bands by the electronic interactions of the participation. of the orbital electrons joined by Nd, that is, red Nd(d) in the vicinity of the Fermi level from -0.5 eV to 0.5 eV and Nd(f) in the conduction band from 0.5 eV to 2eV covering for all four sites studied. Especially in Figure 3, we see the participation of Si(d) electron orbitals in the conduction band when absorption of Nd/ASiNRs occurs, but when in the pristine state, this orbital electron does not participate in the structure. its characteristic Band region architecture.

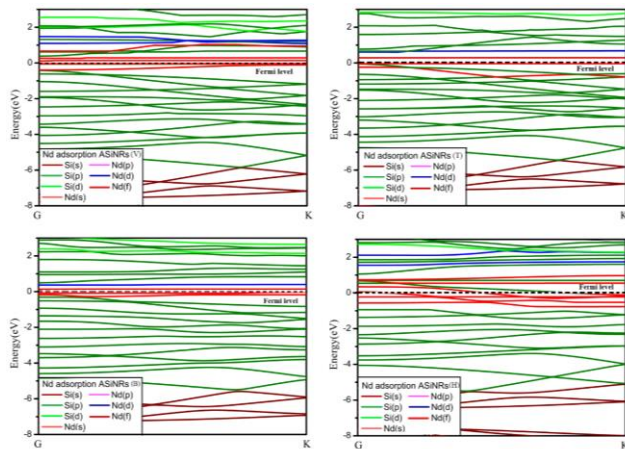


Figure 3 BAND structures of four positions Valley, Top, Bridge, and Hollow

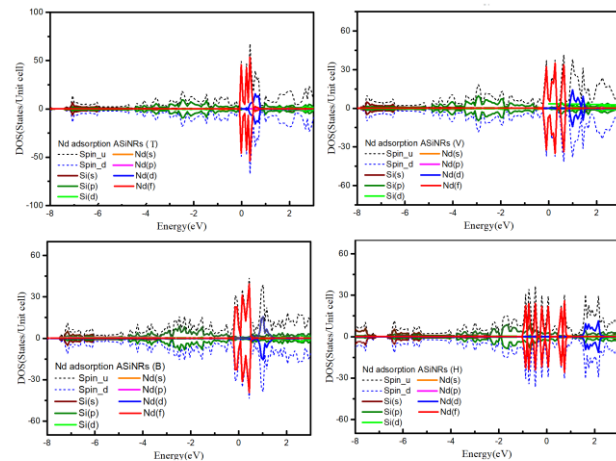


Figure 4 DOS structures of valley, top, bridge, and hollow

In Figure 4, the DOS state density of the top, valley, bridge, and hollow cases we find that they have similarities, similar to that considered on the band in the energy region in Figure 3. However, the participation of Nd(f) electron orbitals in each different case will have different strengths and weaknesses. For the V-Valley position, the Nd(f) electron orbitals mainly appear in the conduction band with energies from -0.2 eV to 1eV and with a strength of about 40 (states/eV). The Nd(f) electron orbital T-Top site is active mainly in the vicinity of Fermi from -0.1 eV to 0.8 eV and the magnitude is relatively large, around 60 (states/eV). For the case at the B-Bridge position, the Nd(f) orbital electrons are concentrated in the conduction band, it operates from -0.3 eV to 0.5 eV and the intensity is also large, the highest is about ~ 45 (states/eV). Particularly for the case at the hollow position, the orbital electrons operate in a very wide range from the top of the valence band to the bottom of the conduction band, the energy is in the range of -1 eV to 1eV and the intensity is also relatively uniform between the electrons. orbit, the amplitude is about ~ 30 (states/eV).

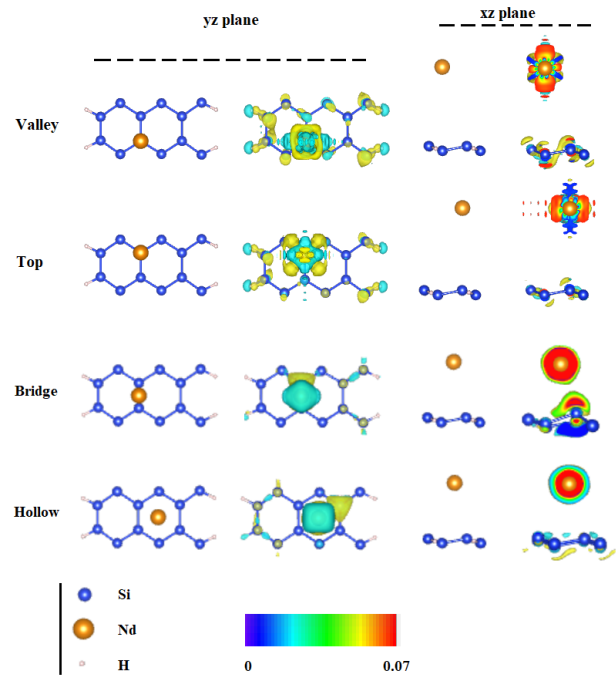


Figure 5 CHARCAR files of 4 positions

By examining the CHGCAR file of Nd absorption cases on the background of ASiNRs at 4 different locations top, valley, hollow, and bridge, we have the results as shown in Figure 5. Considering four different positions from the results of reviewing the structural state of the CONTCAR file (drawn on VESTA software) and looking at the images of the model of the electronic orbitals in the cases shown. When we choose, the charge concentration is shown on the color axis from 0 to 0.07 e/A³ with the color range from B-G-R and plotting the composite files on VESTA we found. To consider the charge displacement during

absorption between the substrate and the metal, we use the following calculation formula:

$$\Delta\rho = \rho_s - \rho_P - \rho_M \quad (2)$$

where ρ_s is the charge density of the system after doping; ρ_P is the charge density of the substrate before doping; ρ_M is the charge density of the doped metal component

The electrons belonging to the Si atoms in the vicinity of the present Nd site tend to participate in more or less charge interactions, the donating and accepting charges of the electron regions are occurring from here, resulting in leads to electron displacement, creating valence band filling and conduction band electrons, ready to move in the presence of an interacting external electric field (which is the general case of the 4 Nd-doped states that all new compounds are metallic, band gap $E_g = 0$).

Looking at the Bridge case of Figure 5, the electrons orbiting around the Nd atom in the Nd(f) orbital state have a very strong charge, which tends to pull the Nd atom toward the pristine substrate ASiNRs. At the same time, the participation of Si(d) electrons leads to more warping than in other cases, specifically, here the degree of Buckl is 0.69 Å compared to Buckl of 0.4 Å (for Top case), and 0.38 Å (Bridge case).

We proceed to consider the electronic transition from Nd atom to ASiNRs and vice versa through specific orbitals by reviewing the calculation results with DFT theory.

Calculation results show that, in the pristine state of silicene, the electron density of the Si(s) atom is 12.66 $e/\text{Å}^3$, Si(p) is 17.0 $e/\text{Å}^3$, Si(d) is 1.24 $e/\text{Å}^3$. The initial Nd atom has an electron density of Nd(s) of 1.96 $e/\text{Å}^3$, Nd(p) of 5.39 $e/\text{Å}^3$, Nd(d) of 0.92 $e/\text{Å}^3$, and Nd(f) of 2.30 $e/\text{Å}^3$. When Nd adsorption occurs on SiNRs, a complex is formed with electron density Sys(s) of 15.28 $e/\text{Å}^3$, Sys(p) of 21.2 $e/\text{Å}^3$ and Sys(d) of 1.18 $e/\text{Å}^3$ and Sys(f) is 5.58 $e/\text{Å}^3$.

Thereby, it shows that when adsorption occurs, the electron charge density in the s orbit increases from 14.62 $e/\text{Å}^3$ to 15.28 $e/\text{Å}^3$, the d orbital electron charge density decreases from 2.16 $e/\text{Å}^3$ down to 1.18 $e/\text{Å}^3$, and the p orbital electron charge density also decreases from 22.39 $e/\text{Å}^3$ to 21.2 $e/\text{Å}^3$. Especially with the f orbital, the electron charge density changes very strongly from 2.3 $e/\text{Å}^3$ up to 5.58 $e/\text{Å}^3$.

4.0 CONCLUSION

In this project, we initially learn about VASP and study some properties and configurations of silicene nanoribbon when doping with Nd, thereby proposing a model to create new electronic materials for the future, applying them used in materials science and engineering science. There are 4 configurations studied: top, valley, bridge, and hollow configuration. The original configuration of SiNRs is a semiconductor

with a band gap of 0.33 eV. After Nd doping, the top, valley, bridge, and hollow configurations all become semi-metallic with Fermi-level cutoff energies, going from the conduction band to the valence band, but without a band gap. The contribution of Si states in the pristine configuration ASiNRs lies in the valence band middle and top for Si(s) and conduction band bottom for Si(p). Between them exists a band gap E_g that is characteristic of a semiconductor. So when doping Nd into ASiNRs with 4 different configurations, the results show: All 4 configurations give the compound-formed semiconducting, magnetic.

Particularly, the Bridge configuration gives the most satisfactory result that is the band gap $E_g=0$ with the stable structure being the lowest absorption energy, the participation of orbital electrons of Nd(f) and Nd(d) is also very powerful in shifting the charge from the valence band to the conduction band. As a result, the substrate ASiNRs turn to metal in the presence of Nd adsorption. The characteristic magnetic moments of doped Nd/ASiNRs have relatively large values, which have the potential to be used to fabricate future devices such as spin motors, and field-effect transistors.

Conflicts of Interest

The author(s) declare(s) that there is no conflict of interest regarding the publication of this paper.

Acknowledgment

This research used resources from the high-performance computer cluster (HPCC) at Thu Dau Mot University (TDMU), Binh Duong Province, Vietnam.

References

- [1] Paola De Padova *et al.* 2012. 1D Graphene-like Silicon Systems: Silicene Nano-ribbons. *Journal of Physics: Condensed Matter*. 24(22): 223001. Doi: 10.1088/0953-8984/24/22/223001.
- [2] S. Sinha *et al.* 2021. Preparation and Application of OD-2D Nanomaterial Hybrid Heterostructures for Energy Applications. *Materialstoday Advances*. 12: 100169. <https://doi.org/10.1016/j.mtadv.2021.100169>.
- [3] Kyozauro Takeda, Kenji Shiraishi. 1994. Theoretical Possibility of Stage Corrugation in Si and Geanalogs of Graphite. *Phys Rev B*. 50: 20. <https://doi.org/10.1103/PhysRevB.50.14916>.
- [4] Mathew, J. Cherukara *et al.* 2017. Silicene Growth through Island Migration and Coalescence, *Nanoscale*. 9: 10186-10192. <https://doi.org/10.1039/C7NR03153J>.
- [5] Maurizio De Crescenzi *et al.* 2016. Formation of Silicene Nanosheets on Graphite. *ACS Nano*. 10(12): 11163-11171. <https://doi.org/10.1021/acsnano.6b06198>.
- [6] Tang, C. *et al.* 2013. Structure-stability Relationships for Graphene-Wrapped Fullerene-coated Carbon Nanotubes. *Carbon*. 61: 458-66. <http://dx.doi.org/10.1016/j.carbon.2013.04.103>.

- [7] Sadeddine, S. *et al.* 2017. Compelling Experimental Evidence of a Dirac Cone in the Electronic Structure of a 2D Silicon Layer. *Sci. Rep.* 7: 44400. <https://doi.org/10.1038/srep44400>.
- [8] Boubekeur Lalmi *et al.* 2012. Epitaxial Growth of a Silicene Sheet. *Applied Physics Letters*. 97(22). <https://doi.org/10.1063/1.3524215>.
- [9] Gogotsi, Y. *et al.* 2019. The Rise of Mxenes. *ACS Nano*. 13: 84914. <https://doi.org/10.1021/acsnano.9b06394>.
- [10] Lima, M. P. *et al.* 2018. Silicene-based FET For Logical Technology. *IEEE Electron Device Lett.* 39: 1258-61. <https://doi.org/10.1149/2162-8777/abd09a>.
- [11] Aghaei, S. M. *et al.* 2016. Theoretical Study of Gas Adsorption on Silicene Nanoribbons and Its Application in a Highly Sensitive Molecule Sensor. *RSC Adv.* 6: 94417-94428. <https://doi.org/10.1039/C6RA21293J>.
- [12] Galashev, A. Y. *et al.* 2020. Silicene Anodes for Lithium-ion Batteries on Metal Substrates. *J. Electrochem. Soc.* 167: 50510. <http://dx.doi.org/10.1149/1945-7111/ab717a>.
- [13] Sadeddine, S. *et al.* 2017. Compelling Experimental Evidence of a Dirac Cone in the Electronic Structure of a 2D Silicon Layer. *Sci. Rep.* 7: 44400. <https://doi.org/10.1038/srep44400>.
- [14] Liu, C-C. *et al.* 2011. Quantum Spin Hall Effect in Silicene and Two-dimensional Germanium. *Phys. Rev. Lett.* 107: 76802. <https://doi.org/10.1103/PhysRevLett.107.076802>.
- [15] Ni, Z. *et al.* 2012. Tunable Band Gap in Silicene and Germanene. *Nano Lett.* 12: 113. <https://doi.org/10.1021/nl203065e>.
- [16] Jia, T-T. *et al.* 2015. Band Gap on/off Switching of Silicene Superlattice. *J. Phys. Chem. C.* 119: 20747. <https://doi.org/10.1021/acs.jpcc.5b06626>.
- [17] Drummond, N. D. *et al.* 2012. Electrically Tunable Band Gap In Silicene. *Phys. Rev. B.* 85: 75423. <https://doi.org/10.1103/PhysRevB.85.075423>.
- [18] Lin, S-Y. *et al.* 2020. Stacking-configuration-enriched fundamental Properties in Bilayer Silicenes, Silicene-based Layer. *Mater.* 5: 28. <https://doi.org/10.48550/arXiv.1912.10257>.
- [19] Jia, T-T. *et al.* 2015. Band Gap on/off Switching of Silicene Superlattice. *J. Phys. Chem. C.* 119: 20747. <https://doi.org/10.1021/acs.jpcc.5b06626>.
- [19] Drummond, N. D., Zólyomi, V. and Fal'ko, V. I. 2012. The Electrically Tunable Band Gap in Silicene. *Phys. Rev. B.* 85: 75423. <https://doi.org/10.1103/PhysRevB.85.075423>.
- [20] A. Fleurence *et al.* 2013. Simultaneous Optimization of Spin Fluctuations and Superconductivity under Pressure in an Iron-Based Superconductor. *Phys. Rev. Lett.* 111: 107004. <https://doi.org/10.1103/PhysRevLett.111.107004>.
- [21] Mehdi, A. *et al.* 2016. Structural Stability of Functionalized Silicene Nanoribbons with Normal, Reconstructed, and Hybrid Edges. *Nanomater.* 59: 59162. <http://dx.doi.org/10.1155/2016/5959162>.
- [22] Chuan, M. W. *et al.* 2019. Electronic Properties of Silicene Nanoribbons using the Tight-binding Approach. *International Symposium on Electronics and Smart Devices (ISESD)*. 1–4. <http://dx.doi.org/10.1109/ISESD.2019.8909598>.
- [23] Daniele Chiappe, *et al.* 2012. Local Electronic Properties of Silicene Phases. *Advanced Materials*. 24(37): 5088-93. <https://doi.org/10.1002/adma.201202100>.
- [24] Ghasemi, N. *et al.* 2019. Electronic, Magnetic and Transport Properties of Zigzag Silicene Nanoribbon Adsorbed with Cu Atom: A First-principles Calculation. *J. Magn. Magn. Mater.* 473: 306-11. <http://dx.doi.org/10.1016/j.jmmm.2018.10.059>.
- [25] Xu, L. *et al.* 2015. Adsorption of Ti Atoms on Zigzag Silicene Nanoribbons: Influence on Electric, Magnetic, and Thermoelectric Properties. *J. Phys. D. Appl. Phys.* 48: 215306. <https://iopscience.iop.org/article/10.1088/0022-3727/48/21/215306>.
- [26] Andrzej, Szytuła. 2020. Handbook of Crystal Structures and Magnetic Properties of Rare Earth Intermetallics. *Physical Sciences*. <http://dx.doi.org/10.1201/9780138719411>.
- [27] Werbowy, S., Windholz, L. 2017. Studies of Landé gJ-Factors of Singly Ionized Neodymium Isotopes (142, 143, and 145) at Relatively Small Magnetic Fields up to 334 G by Collinear Laser Ion Beam Spectroscopy. *Eur. Phys. J. D.* 71:16. <https://doi.org/10.1140/epjd/e2016-70641-3>.
- [28] T. J. Zhang *et al.* 1987. Experimental Study of Electrical Properties at the Nd-doped Si-SiO₂ Interface. *Journal of Physics and Chemistry of Solids*. 48(6): 551-554. [https://doi.org/10.1016/0022-3697\(87\)90050-3](https://doi.org/10.1016/0022-3697(87)90050-3).
- [29] E. Steveler *et al.* 2014. Photoluminescence Properties of Nd-doped Silicon Oxide Thin Films Containing Silicon Nanoparticles. *Journal of Luminescence*. 150: 35-39. <https://doi.org/10.1016/j.jlumin.2014.01.061>.
- [30] Wei-Fan Lee *et al.* 2009. Nd-doped Silicon Nanowires with Room Temperature Ferromagnetism and Infrared Photoemission. *Appl. Phys. Lett.* 94: 263117. <https://doi.org/10.1063/1.3168550>.
- [31] Pavel Straka *et al.* 2019. Linear Structures of Nd-Fe-B Magnets: Simulation, Design and Implementation in Mineral Processing – A Review. *Minerals Engineering*. 143(November 2019): 105900. <https://doi.org/10.1016/j.mineng.2019.105900>.
- [32] A. I. Zagumennyi *et al.* 1992. The Nd:GdVO₄ Crystal: A New Material for Diode-pumped Lasers. *Soviet Journal of Quantum Electronics*. 22(12): 22-1071. <https://iopscience.iop.org/article/10.1070/QE1992v022n12ABEH003672>.
- [33] M. M. Carnasciali *et al.* 1983. Phase Equilibria in the Nd-Cu System. *Journal of the Less Common Metals*. 92(1): 97-103. [https://doi.org/10.1016/0022-5088\(83\)90230-8](https://doi.org/10.1016/0022-5088(83)90230-8).
- [34] Gschneidner, K. A., Calderwood, F. W. 1982. The Er-Nd (Erbium-Neodymium) System. *Bulletin of Alloy Phase Diagrams*. 3: 350-351. <https://doi.org/10.1007/BF02869308>.
- [35] Jirapan Dutchaneephet *et al.* 2018. Optical Spectroscopic Investigations of Neodymium and Erbium Added Bismuth Silicate Glasses. *Optik*. 178: 111-116. <https://doi.org/10.1016/j.ijleo.2018.09.172>.
- [36] Yifeng, Shi *et al.* 2022. Synthesis, Structures, Optical Properties and DFT Studies Of Neodymium Complexes Containing Octanoyl Amino Carboxylic Acids. *Optics & Laser Technology*. 155: 108445. <https://doi.org/10.1016/j.optlastec.2022.108445>.